ISBN: 978-3-95450-227-1 ISSN: 2673-5490 doi:10.18429/JACoW-IPAC2022-TUPOTK005

MITIGATION OF PARASITIC LOSSES IN THE QUADRUPOLE RESONATOR ENABLING DIRECT MEASUREMENTS OF LOW RESIDUAL RESISTANCES OF SRF SAMPLES

S. Keckert*, R. Kleindienst, J. Knobloch[1], F. Kramer, O. Kugeler, D. Tikhonov,
Helmholtz-Zentrum Berlin, Berlin, Germany
[1]also at Universität Siegen, Siegen, Germany
W. Ackermann, H. De Gersem, Technische Universität Darmstadt, Darmstadt, Germany
M. Wenskat, Universität Hamburg, Hamburg, Germany
X. Jiang, A. O. Sezgin, M. Vogel, Universität Siegen, Siegen, Germany

Abstract

The quadrupole resonator (QPR) is a dedicated sample-test cavity for the RF characterization of superconducting samples in a wide temperature, RF field and frequency range. Its main purpose are high resolution measurements of the surface resistance with direct access to the residual resistance thanks to the low frequency of the first operating quadrupole mode. Besides the wellknown high resolution of the QPR, a bias of measurement data towards higher values has been observed, especially at higher harmonic quadrupole modes. Numerical studies show that this can be explained by parasitic RF losses on the adapter flange used to mount samples into the QPR. Coating several micrometer of niobium on those surfaces of the stainless steel flange that are exposed to the RF fields significantly reduced this bias, enabling a direct measurement of a residual resistance smaller than 5 nΩ at 2 K and 413 MHz.

INTRODUCTION

This contribution addresses the key results of our study on parasitic losses in the QPR and their mitigation. For a comprehensive discussion and further details see [1].

The surface resistance of superconducting radio frequency (SRF) cavities is commonly approximated by

$$R_S = R_{BCS} + R_{res} = \frac{af^2}{T} \exp\left(-\frac{\Delta}{k_B T}\right) + R_{res} \qquad (1)$$

with intrinsic BCS resistance (R_{BCS}) and a residual resistance (R_{res}). R_{BCS} depends on a material parameter (a) and the superconducting energy gap (Δ), the contributions to R_{res} are less well understood and are still under investigation. Hence, for R&D on materials, coatings or surface treatments aiming at application in SRF cavities, precision measurements of the surface resistance are required.

The QPR provides high resolution measurements in a wide parameter space of temperature and RF field at three different frequencies [2–5]. With a first operating quadrupole mode at about 415 MHz, R_{BCS} at 2 K is typically smaller than 2 nΩ, enabling direct measurements of R_{res}. Operational experience indicates a bias of measurement data towards a systematically overestimated R_S, limiting the accuracy at low R_S and hence especially impacting R_{res} [6–8].

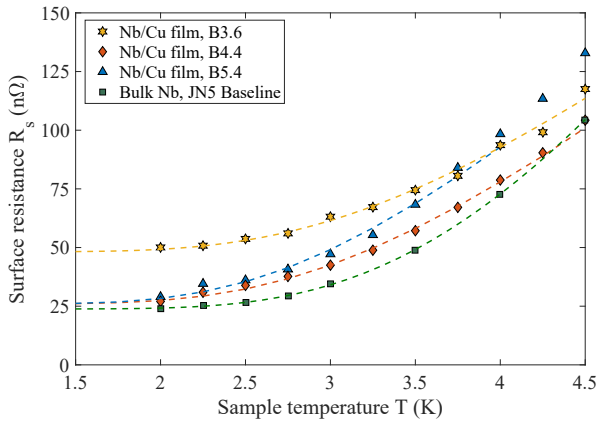

Figure 1: Representative measurement results of different niobium on copper films as well as for a bulk Nb sample at 415 MHz. The BCS resistance is fitted using Eq. (1).

As an example, Fig. 1 shows a series of measurements of R_S vs. temperature for different Nb on copper films as well as for a bulk Nb sample (JN5). The results show that at the first quadrupole mode ($f \approx 415$ MHz), R_{res} is larger than 20 nΩ, even for the bulk niobium sample.

A calorimetric compensation technique is used to derive the sample's R_S at the actively stabilized temperature of interest. Comparing the levels of DC heater power that are required in thermal equilibrium either with or without applied RF field, directly gives the RF dissipated power and hence R_S according to

$$R_S = \frac{2P_{diss}}{\int_{sample} ||H||^2 \, dS} = 2c\frac{\Delta P_{DC}}{P_t Q_t} \qquad (2)$$

with transmitted power P_t, pickup coupling Q_t and calibration constant c. It is important to keep in mind, that any heating occurring in the thermal system of the sample assembly will be interpreted as R_S of the sample.

We will see that the observed behavior of biased R_{res} is dominated by parasitic losses on the normal conducting sample adapter flange. Coating this flange with niobium reduced this bias at the first quadrupole mode by more than 10 nΩ. At 1.3 GHz this improvment is even larger where due to a reduced damping in the coaxial gap a measurement of R_{res} hitherto was impossible.

* sebastian.keckert@helmholtz-berlin.de

ISBN: 978-3-95450-227-1 ISSN: 2673-5490 doi:10.18429/JACoW-IPAC2022-TUPOTK005

NUMERICAL ANALYSIS

The QPR sample chamber assembly consists of a top-hat-shaped superconducting part and a stainless steel adapter flange as shown in Fig. 2. An indium wire provides the vacuum seal separating the inner insulation vacuum of the sample chamber from the resonator volume. The assembled sample chamber is inserted into the QPR from below, acting as an inner conductor of a coaxial line. All flanges are made from stainless steel, all other parts are manufactured from high RRR bulk niobium. Further details about the QPR can be found in [5].

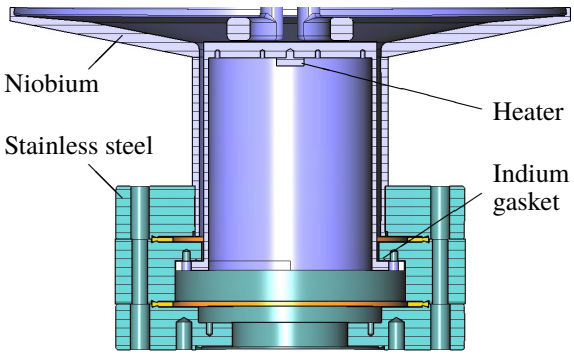

Figure 2: Cross section of the sample assembly mounted into the QPR. The actual sample surface is given by the circular top area positioned at close distance to the QPR pole shoes.

To study possible sources of parasitic losses and their impact on the measurement accuracy, the entire measurement process was translated into a numercial simulation model in CST Studio Suite [9].

First, the surface power density that locally heats up the field-exposed components is determined numerically by eigenvalue calculations. To estimate the contribution of the parasitic heating originating merely from the mounting of the sample into the resonator, the electrical conductivity of niobium at cryogenic temperatures is assumed to be infinitely high compared to the finite values of the surrounding materials (data taken from [10]).

In a second step, the steady-state temperature is calculated. Due to the nonlinear thermal behavior of the underlying materials, this simulation has to be restarted again and again once the magnitude of the RF field has changed. Thermal conductivities of the involved materials are taken from refs. [11, 12]. Based on earlier work, thermal boundary resistances are neglected since measurement data can be reproduced succesfully in simulations with volumetric thermal conductivities only [7]. The superfluid LHe bath surrounding the QPR is modeled using a fixed-temperature boundary condition at 2 K. An exemplary temperature distribution is visualized in Fig. 3.

In step 3, the situation without applied RF field is considered by calculating steady-state temperature distributions from various power excitations of a dedicated heater underneath the sample surface. From the resulting sample temperatures as a function of the excitation power allows the

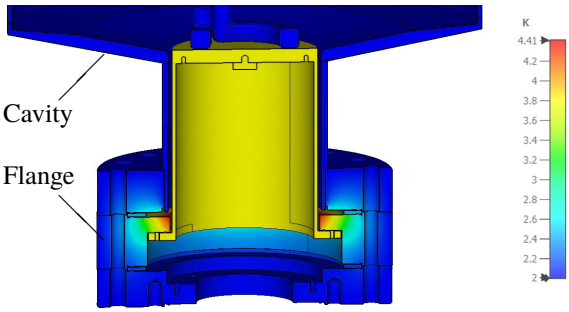

Figure 3: Simulated temperature distribution due to power dissipation on normal conducting materials (flanges and copper and indium seals) in the lower part of the QPR.

effective sample heating power for the different heat sources is obtained, which then allows to quantify the influence of artificial heating in terms of an additional surface resistance originating from parasitic heating effects.

Comparing the baseline scenario with the case of a niobium-coated sample adapter flange (see Fig. 4) indicates that the unacceptable heating of the sample is mainly attributed to a few surfaces that are easily accessible for coatings without the need for a major rework of the resonator itself. For further details see [1].

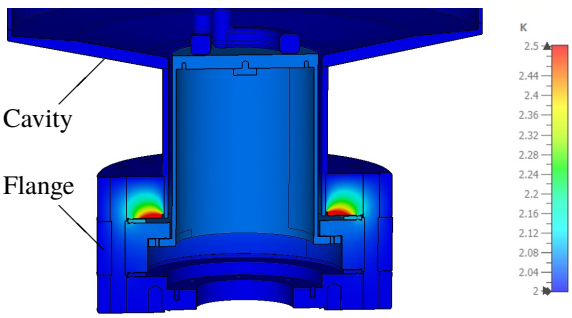

Figure 4: Simulated temperature distribution for the case of a niobium coated sample adapter flange.

SAMPLE AND FLANGE PREPARATION

The sample tested in this study consists of a bulk copper substrate coated with 45 µm of niobium by DC magnetron sputtering at INFN Legnaro [13].

The adapter flange used to mount the sample into the QPR is a double-side CF100 flange from 1.4429-ESU (316LN ESR) material. After the baseline measurement, the flange was coated by high power impulse magnetron sputtering (HiPIMS) at a temperature of 400 °C and a sample bias of −50 V DC at the University of Siegen. The resulting niobium coating thickness is approximately 12 µm.

SURFACE RESISTANCE MEASUREMENTS

Measurement data of the exact same sample before and after coating the adapter flange is shown in Fig. 5. All datasets of R_S vs. RF field (at constant temperature) show a "jump"

ISBN: 978-3-95450-227-1 ISSN: 2673-5490 doi:10.18429/JACoW-IPAC2022-TUPOTK005

in R_S at about 30 mT. The field level at which the jump occurs depends weakly on temperature, while the amplitude remains constant. This can be interpreted as a "Q-switch" behavior of the sample, independent of the adapter flange [14]. The visible "jump" in R_S data at the same field level and with the same amplitude for baseline and Nb coated flange test excludes significant errors coming from the RF measurements or possible mounting issues.

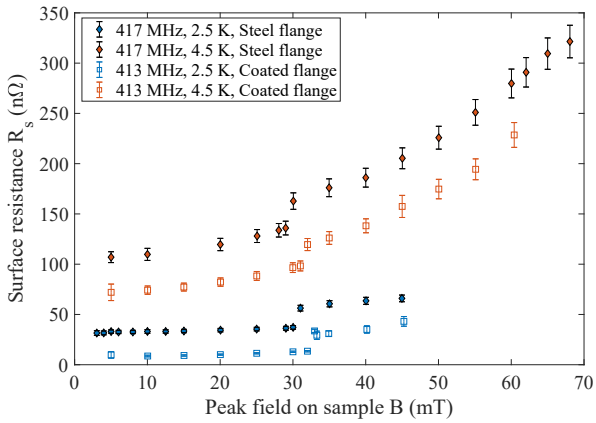

Figure 5: Surface resistance vs. RF field results for the baseline and the Nb coated flange test at different temperatures.

Thanks to the strong suppression of RF dissipation on the niobium coated adapter flange, especially at higher frequencies, measurements of R_S were possible at all three quadrupole modes at temperatures down to 2 K. Measurement data taken at a constant level of RF field together with fits extrapolating R_{res} according to Eq. (1) is shown in Fig. 6. Fit results for baseline measurement and the test with niobium coated flange are given in Table 1. Note that thanks to the low frequency of about 415 MHz and sample temperatures down to 2 K the uncertainty in R_{res} is less than 1 nΩ. Baseline values for R_S of about 25 – 30 nΩ at the first quadrupole mode near 415 MHz are typical values, also compared to other samples (see Fig. 1).

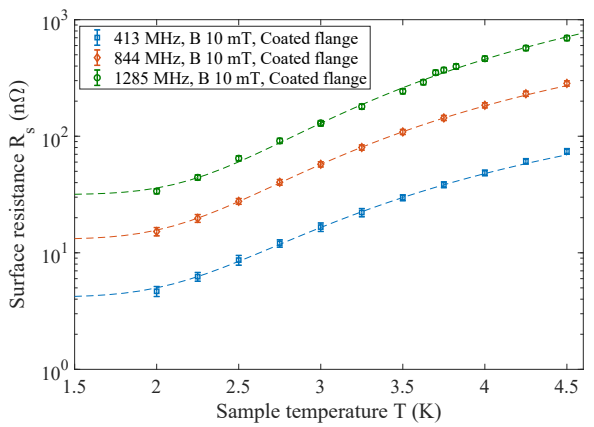

Figure 6: R_S vs. T for the coated flange at three quadrupole modes. R_{res} is extrapolated from fits using Eq. (1).

Table 1: R_{res} Obtained from Fitting and Selected R_S Data, In All Cases an RF Field Level of 10 mT was Applied

Setup	Freq.	R_S (2.0 K)	R_S (4.5 K)	R_{res}
Baseline	413 MHz	28.7 nΩ	110 nΩ	28.5 nΩ
niobium	417 MHz	4.7 nΩ	74.2 nΩ	4.2 nΩ
coated	844 MHz	15.2 nΩ	284 nΩ	13.1 nΩ
flange	1285 MHz	33.8 nΩ	696 nΩ	31.6 nΩ

CONCLUSION

This study clearly shows that the application of a superconducting niobium coating on the stainless steel adapter flange at the far end of the coaxial gap between quadrupole resonator and QPR sample solved the problem with systematic errors from which the QPR suffered in the past. The R_S vs. T measurement with the Nb-coated adapter flange shows a reduction by 24 nΩ over the entire temperature range at the first quadrupole mode. The measured R_S values are now comparable with the ones obtained in SRF cavity measurements. Up to now, no sample-test cavity has demonstrated absolute R_S values lower than 5 nΩ. At the third quadrupole mode R_S values lower than 35 nΩ have been achieved, boosting the accuracy of the QPR to an unprecedented level.

The measurements of R_S vs. RF magnetic field show that the error in R_S – originating from parasitic losses in the stainless steel adapter flange – is nearly independent of temperature and RF field strength (see Fig. 5). This was expected from the numerical simulations because the dissipated power depends quadratically on the RF field amplitude for both, superconductors and normal conductors. Hence, the contribution of parasitic losses to the observed R_S mainly affects the measurement accuracy of R_{res} and can be treated as a systematic bias. On a side note, the measurement precision, i.e. the reproducibility, has always been very good, and was not further improved by the flange coating. It is conceivable that a dependence on temperature or RF field amplitude could originate from temperature dependent thermal conductivities, however, this would only be a second-order effect and could not explain the measured data.

Establishing coated flanges as a new standard for QPR samples opens up new possibilities for the RF characterization of superconducting samples, e.g. investigating possibly frequency dependent R_{res}.

ACKNOWLEDGEMENTS

We thank V. Garcia Diaz, E. Chyhyrynets and C. Pira (INFN Legnaro, Italy) for supplying the niobium thick-film QPR sample which has received funding from the European Union's Horizon 2020 Research and Innovation programme under Grant Agreement No 101004730.

We would like to express our gratitude to the SMART collaboration – coordinated by the spokesperson W. Hillert (Universität Hamburg) – for many fruitful discussions. This research has been funded by the Federal Ministry of Education and Research of Germany (BMBF), project number 05K2019 - SMART.

ISBN: 978-3-95450-227-1 ISSN: 2673-5490 doi:10.18429/JACoW-IPAC2022-TUPOTK005

REFERENCES

[1] S. Keckert *et al.*, "Mitigation of parasitic losses in the quadrupole resonator enabling direct measurements of low residual resistances of srf samples," *AIP Advances*, vol. 11, no. 12, p. 125 326, 2021, doi:10.1063/5.0076715

[2] E. Chiaveri, E. Haebel, E. Mahner, and J. M. Tessier, "The Quadrupole Resonator, Construction, RF System, Field Calculations and First Applications," in *Proc. EPAC'98*, Stockholm, Sweden, Jun. 1998, https://jacow.org/e98/papers/TUP041B.pdf

[3] E. Mahner, S. Calatroni, E. Chiaveri, E. Haebel, and J. M. Tessier, "A new instrument to measure the surface resistance of superconducting samples at 400 MHz," *Review of Scientific Instruments*, vol. 74, no. 7, pp. 3390–3394, 2003, doi:10.1063/1.1578157

[4] T. Junginger, W. Weingarten, and C. Welsch, "Extension of the measurement capabilities of the quadrupole resonator," *Review of Scientific Instruments*, vol. 83, no. 6, p. 063 902, 2012, doi:10.1063/1.4725521

[5] S. Keckert, R. Kleindienst, O. Kugeler, D. Tikhonov, and J. Knobloch, "Characterizing materials for superconducting radiofrequency applications — a comprehensive overview of the quadrupole resonator design and measurement capabilities," *Review of Scientific Instruments*, vol. 92, no. 6, p. 064 710, 2021, doi:10.1063/5.0046971

[6] R. Kleindienst, *Radio Frequency Characterization of Superconductors for Particle Accelerators*. Universität Siegen, 2017, Dissertation, http://dokumentix.ub.uni-siegen.de/opus/volltexte/2018/1329/.

[7] S. Keckert, *Characterization of Nb_3Sn and Multilayer Thin Films for SRF Applications*. Universität Siegen, 2019, Dissertation, doi:10.25819/ubsi/1487

[8] S. Keckert, T. Junginger, J. Knobloch, and O. Kugeler, "The Challenge to Measure nanoohm Surface Resistance on SRF Samples," in *Proc. IPAC'18*, Vancouver, Canada, Apr.-May 2018, pp. 2812–2815, doi:10.18429/JACoW-IPAC2018-WEPML049

[9] Dassault Systèmes, *CST Studio Suite*, version 2021 SP5, https://www.3ds.com

[10] M. Merio, "Material properties for engineering analysis of srf cavities," Fermilab Technical Division Department, Batavia, Illinois, Tech. Rep., 2013, 5500.000-ES-371110 Rev. A.

[11] F. Koechlin and B. Bonin, "Parametrization of the niobium thermal conductivity in the superconducting state," *Superconductor Science and Technology*, vol. 9, no. 6, pp. 453–460, 1996, doi:10.1088/0953-2048/9/6/003

[12] NIST Standard Reference Data project, National Institute of Standards and Technology, https://trc.nist.gov/cryogenics/index.html/.

[13] V. G. Diaz *et al.*, "Thick Film Morphology and SC Characterizations of 6 GHz Nb/Cu Cavities," in *Proc. SRF'21*, East Lansing, MI, USA, pp. 18–22, doi:10.18429/JACoW-SRF2021-SUPCAV007

[14] H. Padamsee, J. Knobloch, and T. Hays, *RF Superconductivity for Accelerators*. Wiley, 2008, 2nd edition.